THE JOURNAL OF BIOLOGICAL CHEMISTRY
Vol. 280, No. 18, Issue of May 6, pp. 17678–17686, 2005

Printed in U.S.A.

Specific Kinetic Alterations of Human $Ca_V2.1$ Calcium Channels Produced by Mutation S218L Causing Familial Hemiplegic Migraine and Delayed Cerebral Edema and Coma after Minor Head Trauma*

Received for publication, January 31, 2005, and in revised form, February 25, 2005
Published, JBC Papers in Press, March 2, 2005, DOI 10.1074/jbc.M501110200

Angelita Tottene‡§, Francesca Pivotto‡§, Tommaso Fellin‡, Tiziana Cesetti‡, Arn M. J. M. van den Maagdenberg¶‖, and Daniela Pietrobon‡**

From the ‡Department of Biomedical Sciences, University of Padova, CNR Institute of Neuroscience, Viale G. Colombo 3, 35121 Padova, Italy, the ¶Department of Human Genetics, Leiden University Medical Center, Wassenaarseweg 72, 2333 AL Leiden, The Netherlands, and the ‖Department of Neurology, Leiden University Medical Center, P. O. Box 9600, 2300 RC Leiden, The Netherlands

Mutation S218L in the $Ca_V2.1$ α_1 subunit of P/Q-type Ca^{2+} channels produces a severe clinical phenotype in which typical attacks of familial hemiplegic migraine (FHM) triggered by minor head trauma are followed, after a lucid interval, by deep (even fatal) coma and long lasting severe cerebral edema. We investigated the functional consequences of this mutation on human $Ca_V2.1$ channels expressed in human embryonic kidney 293 cells and in neurons from $Ca_V2.1$ $\alpha_1^{-/-}$ mice by combining single channel and whole cell patch clamp recordings. Mutation S218L produced a shift to lower voltages of the single channel activation curve and a consequent increase of both single channel and whole cell Ba^{2+} influx in both neurons and human embryonic kidney 293 cells. Compared with the other FHM-1 mutants, the S218L shows one of the largest gains of function, especially for small depolarizations, which are insufficient to open the wild-type channel. S218L channels open at voltages close to the resting potential of many neurons. Moreover, the S218L mutation has unique effects on the kinetics of inactivation of the channel because it introduces a large component of current that inactivates very slowly, and it increases the rate of recovery from inactivation. During long depolarizations at voltages that are attained during cortical spreading depression, the extent of inactivation of the S218L channel is considerably smaller than that of the wild-type channel. We discuss how the unique combination of a particularly slow inactivation during cortical spreading depression and a particularly low threshold of channel activation might lead to delayed severe cerebral edema and coma after minor head trauma.

Familial hemiplegic migraine (FHM)[1] is a rare autosomal dominant subtype of migraine with aura. Apart from the characteristic transient hemiparesis, typical attacks of FHM are similar to those of the common migraine with aura (1). Some FHM patients also show atypical attacks, either with a prolonged aura or with signs of diffuse encephalopathy; moreover, 20% of FHM families show permanent cerebellar symptoms (2). In about half of the families, FHM is caused by missense mutations in the *CACNA1A* gene, encoding the pore-forming α_1 subunit of voltage-gated neuronal $Ca_V2.1$ (P/Q-type) Ca^{2+} channels (FHM-1) (3). $Ca_V2.1$ channels are located at presynaptic terminals and somatodendritic membranes (4) and are expressed in all brain structures that have been implicated in the pathogenesis of migraine (5). They play a prominent role in controlling neurotransmitter release (6) and also exert postsynaptic effects, such as on neuronal excitability (7).

17 different missense mutations have been associated with FHM-1 (8–10). The functional consequences of 10 mutations have been investigated by expressing $Ca_V2.1$ channel subunits in heterologous systems (11–15). Because $Ca_V2.1$ channel expression is almost exclusively restricted to neuronal cells, 4 of these mutations have also been analyzed in neurons from $Ca_V2.1$ $\alpha_1^{-/-}$ mice expressing human $Ca_V2.1$ α_1 subunits (13, 16). Recently, the generation of a knock-in mouse carrying the R192Q FHM-1 mutation allowed the first analysis of mutant channels expressed at their endogenous level in neurons (17). In transfected cells, a consistent effect of FHM-1 mutations was to increase Ca^{2+} influx through single human $Ca_V2.1$ channels in a broad voltage range as a consequence of an increased channel open probability mainly because of a shift to lower voltages of channel activation (13, 14). The consistent gain of function of single mutant $Ca_V2.1$ channels did not result in a consistent increase in whole cell Ca^{2+} current density because the mutations also altered the density of functional channels in the membrane, producing a decrease of whole cell current density at high voltages in transfected neurons and variable effects in HEK293 cells (13, 14, 16). However, in agreement with the gain-of-function phenotype of human $Ca_V2.1$ channels, the P/Q current density in neurons of the R192Q knock-in mouse was larger than in wild-type neurons in a broad voltage range and similar to the wild-type at higher voltages (17). The knock-in mouse also showed increased neurotransmission at the neuromuscular junction and increased susceptibility to cortical spreading depression (CSD), the phenomenon underlying migraine aura (5, 17).

Mutation S218L in the IS4-IS5 loop of the $Ca_V2.1$ α_1 subunit produces a severe clinical phenotype in which typical attacks of FHM triggered by minor head trauma are frequently followed, after a lucid interval, by deep (even fatal) coma or profound stupor, high fever, and long lasting severe cerebral edema (18,

* This work was supported by Telethon-Italy (Grant E1297), the Italian Ministry of University and Research (Grants Prin2003, FIRB2002, St-L449/97, Fondo Integrativo Speciale per la Ricerca), and the European Community (EUROHEAD Grant LSHM-CT-2004-504837). The costs of publication of this article were defrayed in part by the payment of page charges. This article must therefore be hereby marked "*advertisement*" in accordance with 18 U.S.C. Section 1734 solely to indicate this fact.

§ These authors contributed equally to this work.
** To whom correspondence should be addressed. Tel.: 39-49-827-6052; Fax: 39-49-827-6049; E-mail: daniela.pietrobon@unipd.it.

[1] The abbreviations used are: FHM, familial hemiplegic migraine; CSD, cortical spreading depression; GFP, green fluorescent protein; HEK, human embryonic kidney; *i*, single channel current; NMDA, *N*-methyl-D-aspartate; pF, picofarads; p_o, open probability; SL, S218L; TEA, tetraethylammonium; WT, wild-type.

19). Here, we studied the unknown functional consequences of this mutation on human $Ca_V2.1$ channels expressed in HEK293 cells and in neurons from $Ca_V2.1$ $\alpha_1^{-/-}$ mice and asked the question: with respect to the other FHM-1 mutations, are there some specific effects of S218L which may account for the clinical phenotype of delayed severe cerebral edema and coma after minor head trauma?

MATERIALS AND METHODS

Generation of $Ca_v2.1$ S218L Mutant—The S218L mutation was introduced into the human full-length cDNA (GenBank accession number AF004883) encoding the $Ca_V2.1$ α_1 subunit, cloned in expression plasmid pGFP-, described in Refs. 13 and 20. This human $Ca_V2.1$ α_1 subunit lacks Val^{726}-Ala^{728} and differs in this respect from the cDNA used in Ref. 14. Briefly, mutant PCR products harboring mutation S218L were generated by the "gene SOEing" technique (21). In the first round of PCR, products were generated using either primers 160 (5′-GAACCATACTTCATTGGAAT-3′) and R-S218L (5′-TGATC**A**ACTTCAGGACGACTTGTAA-3′) (250 bp) or F-S218L (5′-TTACAAGTCGTCCTGAAGT**T**GATCATGAAGGCGAT-3′) and 62 (5′-TGAATTCTGCATAGTAAAGG-3′) (939 bp) using proofreading DNA polymerase (*Pfu* Turbo, Stratagene) and $Ca_V2.1$ α_1 subunit cDNA as a template. The C → T nucleotide transversion (at position 889; G → A in the reverse (R-S218L) primer) resulting in a S218L amino acid change is indicated in bold in the primer sequences. Subsequently, a PCR was performed using first round PCR products in combination with primers 160 and 62. Next, this 1,164-bp product containing the S218L (SL) mutation was digested with NotI (nucleotide 838)-StuI (nucleotide 1699) and cloned into NotI-StuI-digested vector pGFP-, resulting in mutant SL. Sequences of the introduced PCR fragment were verified by means of a fluorescent ABI BigDye Terminator Cycle sequencing kit (Applied Biosystems, Foster City, CA). Nucleotide positions corresponding to AF004883 are given. For transfections, plasmid DNA of $Ca_V2.1$ α_1 subunit wild-type (WT) or S218L mutant cDNA was isolated using a QIAfilter Plasmid Maxi kit (Qiagen, Los Angeles, CA).

Cell Culture and Transfection—HEK293 cells were grown and cotransfected with human $Ca_V2.1$ α_1, β_{2e}, or β_{1b} and $\alpha_{2b}\delta$ cDNAs, as described in Ref. 14. Cerebellar granule cells were grown in primary culture from 6-day-old $Ca_V2.1$ $\alpha_1^{-/-}$ mice as described previously (22). Cells were transfected with WT or mutant human $Ca_V2.1$ α_1 cDNA, at days 2 or 3 in culture, using a modified calcium phosphate procedure, as described in Ref. 13. Experiments were performed 1 or 2 days after transfection.

Patch Clamp Recordings and Data Analysis—Whole cell and single channel patch clamp recordings were performed as in Ref. 13. Currents were sampled at 5 kHz and low pass filtered at 1 kHz.

Solutions for whole cell recordings of Ba^{2+} currents in both HEK293 cells and neurons were as follows. The external solution (in mM) was 5 $BaCl_2$, 148 tetraethylammonium (TEA)-Cl, 10 HEPES (pH 7.4 with TEA-OH) (and 5 μM nimodipine and 0.1 mg/ml cytochrome *c*, when recording from neurons). The internal solution (in mM) was 100 cesium methanesulfonate, 5 $MgCl_2$, 30 HEPES, 10 EGTA, 4 ATP, 0.5 GTP, and 1 cAMP (pH 7.4 with CsOH). Solutions for whole cell recordings of Ca^{2+} currents in HEK293 cells were as follows. The external solution (in mM) was 2 $CaCl_2$, 140 TEA-methanesulfonate, 10 HEPES (pH 7.4 with TEA-OH). The internal solution (in mM) was 119 cesium methanesulfonate, 5 $MgCl_2$, 30 HEPES, 0.5 EGTA, 4 ATP, 0.5 GTP and 1 cAMP (pH 7.4 with CsOH). Cells were placed into a recording chamber containing Tyrode's solution and, after attainment of the whole cell configuration, were perfused with the external recording solution.

Compensation (typically 70–80%) for series resistance was used. Current-voltage (*I-V*) curves were obtained only from cells with a voltage error < 5 mV and, in the case of neurons, without signs of inadequate space clamping. The average normalized *I-V* curves were then multiplied by the average maximal current density obtained from all cells. *I-V* curves in HEK293 cells were obtained with voltage ramps (0.85 mV/ms) from a holding potential of −80 mV. *I-V* ramps for leak subtraction were obtained after blockade of Ca^{2+} channels with 5 mM Ni^{2+}. *I-V* curves were fitted with Equation 1.

$$1 = G(V - E_{rev})(1 + \exp((V_{1/2} - V)/k))^{-1} \quad \text{(Eq. 1)}$$

In recording Ba^{2+} currents during long depolarizations in HEK293 cells we noticed a slow progressive increase in the rate of inactivation. Although the mechanism remains unknown, we were very careful in measuring the different properties of inactivation of WT and mutant S218L channels at similar times after breaking into whole cell. Thus the current traces during 1-s depolarizations and the recovery from inactivation were all measured in the time window from 6 to 12 min after whole cell breaking, whereas the currents during 5-s depolarizations and during a train of pulses were measured between 12 and 18 min after whole cell breaking.

Single channel recordings on HEK293 cells were obtained in cell-attached configuration. The pipette solution (in mM) was 90 $BaCl_2$, 10 TEA-Cl, 15 CsCl, 10 HEPES (pH 7.4 with TEA-OH). The bath solution (in mM) was 140 potassium gluconate, 5 EGTA, 35 D-glucose, 10 HEPES (pH 7.4 with KOH). Single channel currents and open probabilities were obtained as in Ref. 14.

The density of functional channels in the membrane for mutant S218L (SL) relative to that of WT channels in HEK293 cells was obtained from Equation 2,

$$N_{SL}/N_{WT} = (I_{SL}/I_{WT})/(i_{SL}p_{oSL}/i_{WT}p_{oWT}) \quad \text{(Eq. 2)}$$

with the whole cell current densities, I_{SL} and I_{WT}, and the products of single channel current and open probability, $i_{SL}p_{oSL}$ and $i_{WT}p_{oWT}$, measured at the peak of the *I-V* and ip_o-*V* curves obtained for mutant and WT channels, respectively.

In both whole cell and single channel recordings the liquid junction potentials were such that a value of 12 mV should be subtracted from all voltages to obtain the correct values of membrane potential (23). Averages are given ± S.E.

RESULTS

In transfected cells expressing human $Ca_V2.1$ channels, a consistent effect of the seven FHM-1 mutations analyzed at the single channel level (T666M, R192Q, V714A, V1457L, I1811L (13, 14), D715E, and I1710T)[2] was to increase the single channel Ca^{2+} influx, as measured by the product of single channel current, *i*, and open probability, p_o, in a broad voltage range (13). Therefore, to investigate whether the functional consequences of mutation S218L were or were not similar to those of typical FHM-1 mutations, first of all, we performed cell-attached single channel recordings on HEK293 cells transfected with human $Ca_V2.1$ α_1 subunits containing mutation S218L and human $\alpha_{2b}\delta$ and β_{2e} subunits and measured *i* and p_o of the mutant channels as a function of voltage.

Fig. 1 compares representative traces of single channel activity at 20 and 30 mV (with 90 mM Ba^{2+} as charge carrier) and the *i-V*, p_o-*V*, and ip_o-*V* relationships obtained for the wild-type and the S218L mutant channels. Mutation S218L did not significantly affect the single channel current and conductance, which was 19.6 ± 0.2 picosiemens (n = 19) for WT and 19.2 ± 0.3 picosiemens (n = 14) for the mutant (Fig. 1*B*). However, the mutation favored the sojourn of the channel in subconductance states, which were rarely observed for the WT channel (see *inset* in Fig. 1*B*). Moreover, the S218L mutation produced a shift of the single channel activation curve toward lower voltages and a consequent increase of the channel open probability in a broad voltage range (Fig. 1*C*). The voltage of half-maximal activation $V_{1/2}$ (obtained by fitting the p_o-*V* relationship with a Boltzmann function) changed from the WT value of 34.1 ± 1 mV (n = 12) to 23.8 ± 1.8 mV (n = 10) for the mutant. Compared with the human FHM-1 mutants whose p_o-*V* relationship was measured previously (13, 14), the S218L is one of the mutants that activates at lower voltages (similar to those of the V714A mutant). Because some of the FHM-1 mutations, including V714A, decreased the unitary current and conductance, we considered the product ip_o (the amount of Ba^{2+} ions entering through a single channel in a given time, *i.e.* the single channel Ba^{2+} influx) as a measure of the gain of function produced by the FHM-1 mutations at the single channel level (13). Fig. 1*D* shows that the single channel Ba^{2+} influx of the S218L mutant is much larger than that of the WT channel in a broad voltage range and similar to that of WT at higher volt-

[2] T. Fellin and D. Pietrobon, unpublished observations.

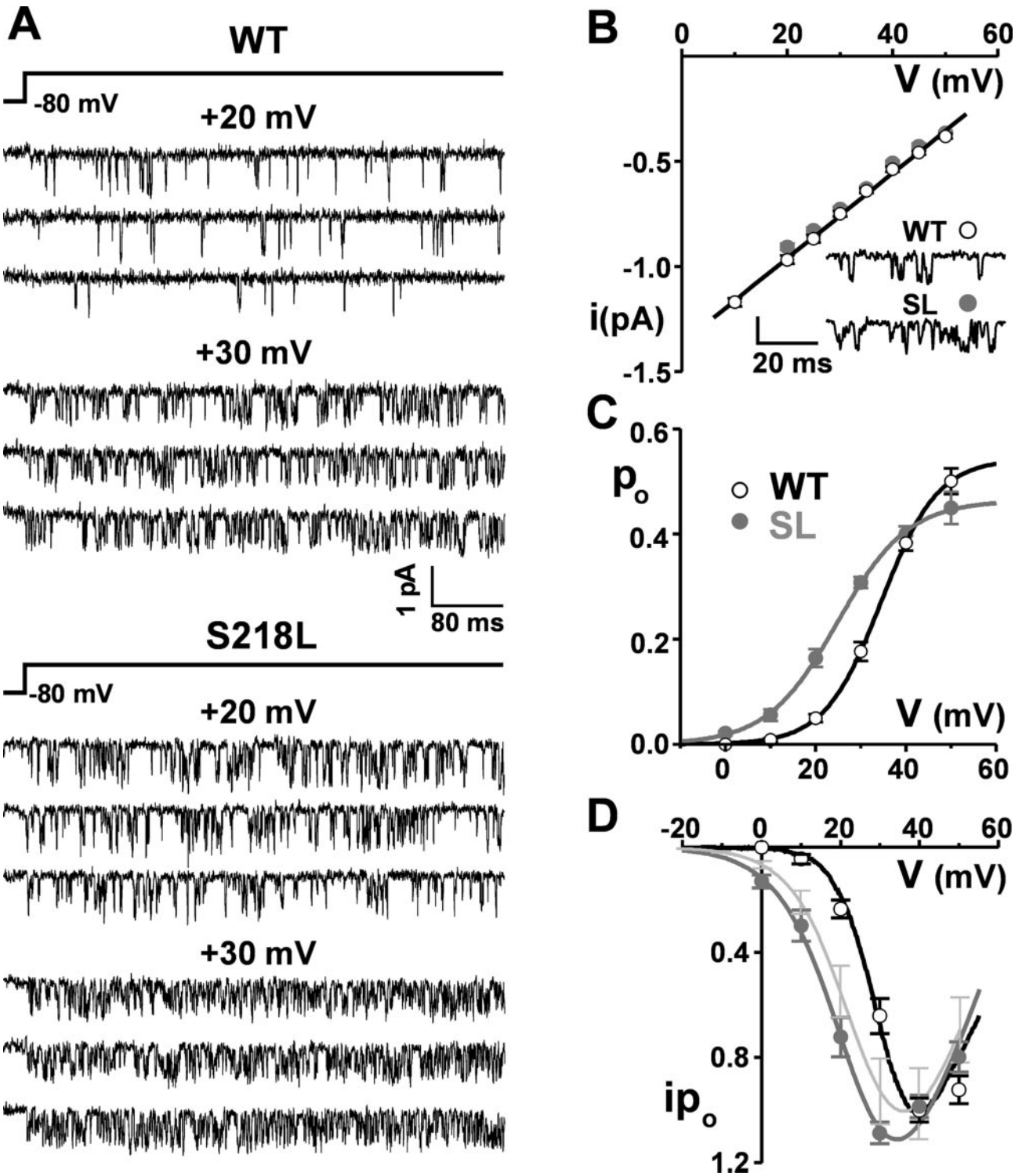

FIG. 1. **Mutation S218L leads to an increased Ba^{2+} influx through single human $Ca_V2.1$ channels by shifting their activation curve toward lower voltages and increasing their open probability.** Single channel cell-attached recordings (90 mM Ba^{2+} as charge carrier) were performed on HEK293 cells cotransfected with human WT or mutant S218L $Ca_V2.1$ α_1 subunits together with human $\alpha_{2b}\delta$ and β_{2e} subunits. Holding potential = −80 mV. *A*, representative current traces at 20 and 30 mV from single channel patches containing a WT $Ca_V2.1$ channel or a S218L mutant. *B*, unitary current, *i*, as a function of voltage for WT and mutant $Ca_V2.1$ channels. *Inset*, unitary activity at 20 mV on an expanded time scale (*scale bars*, 1 pA and 20 ms). Unitary current values are averages from 19 (WT) and 14 (SL) patches. The values of *i* refer to the prevailing larger current level shown in the *inset*. In contrast with the WT, the mutant showed frequent short lived subconductance states. The slope conductances of the average *i-V* relationships were 20 and 19 picosiemens for the WT and the mutant, respectively. *C*, open probability, p_o, as a function of voltage for WT and mutant $Ca_V2.1$ channels; p_o values are averages from 12 (WT) and 10 (SL) patches containing only one channel. The data points were best fitted by Boltzmann distributions of the form $p_o = p_{omx}(1 + \exp(V_{1/2} - V)/k)^{-1}$ with $V_{1/2}$ = 34.5 mV (k = 6.2, p_{omx} = 0.54) for WT and $V_{1/2}$ = 24.8 mV (k = 7.8, p_{omx} = 0.46) for S218L. *D*, product of *i* and p_o as a function of voltage for WT and S218L mutant $Ca_V2.1$ channels. All ip_o values were divided by the maximal ip_o value of the WT channel (−0.21 ± 0.01 pA). The *thin gray line* was obtained by averaging the curves best fitting the voltage dependence of the ip_o values of five FHM-1 mutants (R192Q, T666M, V714A, V1457L and I1815L) taken from (13). The ip_o product reflects the average number of Ba^{2+} ions entering through a single channel in a given time, *i.e.* the single channel Ba^{2+} influx. The normalized ip_o values of the WT channel were well fitted by the normalized whole cell *I-V* curve (Fig. 2) shifted by 26 mV toward more positive voltages (*thick line*). This shift accounts for the difference in surface potential in the single channel and whole cell solutions (90 *versus* 5 mM Ba^{2+}).

ages. It also shows that the gain of function in terms of the single channel Ba^{2+} influx of the S218L mutant tends to be larger than the average gain of function of the human FHM-1 mutants analyzed previously. The difference with respect to the average appears significant at low voltages, where the WT human $Ca_V2.1$ channel remains closed.

The whole cell current-voltage (*I-V*) relationship (with 5 mM Ba^{2+} as charge carrier) revealed a hyperpolarized shift of the voltage range of activation of the mutant channel similar to that measured with single channel recordings (Fig. 2*A*). Fitting of the normalized *I-V* curves obtained with voltage ramps gave $V_{1/2}$ values of +5.0 and −5.7 mV for the WT and the S218L mutant, respectively. Thus, confirming previous findings (13), the effect of the mutation on channel activation appears independent of permeant ion concentration (but note the shift toward lower voltages for both WT and mutant channels because of the larger surface potential at 5 with respect to 90 mM Ba^{2+}). The channel selectivity was not affected by the mutation because the reversal potential of the whole cell current was identical for the WT and mutant channel.

The activation at lower voltages and increased open probability of the mutant channel led to an increased whole cell current density at $V < 0$ mV in HEK293 cells expressing the mutant with respect to those expressing the WT channel (Fig. 2*B*). However, at higher voltages the whole cell current density in cells expressing the mutant was smaller, and the maximal current density was 40% smaller for the mutant than for the WT: 43.2 ± 8 pA/pF (n = 26) *versus* 71.6 ± 11.3 pA/pF (n = 31) (Fig. 2*B*). Given the identical unitary conductance and similar maximal p_o (p_{omx}) of WT and S218L channels (Fig. 1), the reduced current density of the mutant at $V > 5$ mV must be mainly because of a reduced density of functional channels in the membrane. Considering the values of the ip_o product measured at the peaks of the ip_o-*V* curves obtained for the mutant and WT channel and Equation 2 under "Materials and Methods," one obtains a 46 (± 14)% reduction of functional channels in the membrane of cells expressing the mutant. A similar value was obtained by simply considering the ratio of the mutant and WT current densities at voltages where the open probability of both WT and mutant channel reaches the maximum value, and therefore the ratio becomes nearly voltage-independent ($V \geq 20$ mV in Fig. 2*C* $(I_{SL}/I_{WT})_{sat}$ = 0.45). Given that

$$(I_{SL}/I_{WT})_{sat} = (Nip_{omx})_{SL}/(Nip_{omx})_{WT} \quad \text{(Eq. 3)}$$

and that WT and mutant channels have identical single channel current, i, one obtains N_{SL}/N_{WT} = 0.53 (considering $p_{omx,SL}/p_{omx,WT}$ = 0.85 as in Fig. 1*C*) or N_{SL}/N_{WT} = 0.45 (considering not significant the small difference in p_{omx} of WT and mutant in Fig. 1*C*). A reduced density of functional channels in the membrane of HEK293 cells was found for most of the human FHM-1 mutants analyzed previously (13, 14), with the exception of two, which had the opposite effects (R192Q (14) and D715E[2]).

To study the neuronal phenotype of the S218L mutation, we expressed WT and mutant human $Ca_V2.1$ α_1 subunits in cerebellar granule cells in primary culture from $Ca_V2.1$ $\alpha_1^{-/-}$ mice and compared the $Ca_V2.1$ current density measured in these transfected neurons, as done previously for four FHM-1 mutants (13). The $Ca_V2.1$ current density was obtained from the amount of whole cell current inhibited by ω-conotoxin MVIIC applied after the specific blocker of N-type channels ω-conotoxin GVIA (Fig. 3*A*). As a consequence of the shifted activation to lower voltages of mutant channels, the $Ca_V2.1$ whole cell current density in neurons expressing the S218L mutant was larger than that in neurons expressing the WT channel in a broad voltage (Fig. 3*B*). Fitting of the normalized *I-V* curves gave $V_{1/2}$ values of −19.5 mV for the WT channel and of −28.3 mV for the S218L mutant. Taking into account that to correct for junction potentials one should add −12 mV to all the voltages in Fig. 3*B* (*cf.* "Materials and Methods"), our data show that mutant S218L channels can open and carry significant current at voltages (−60 to −50 mV) close to the resting potential of many neurons, where WT channels remain closed.

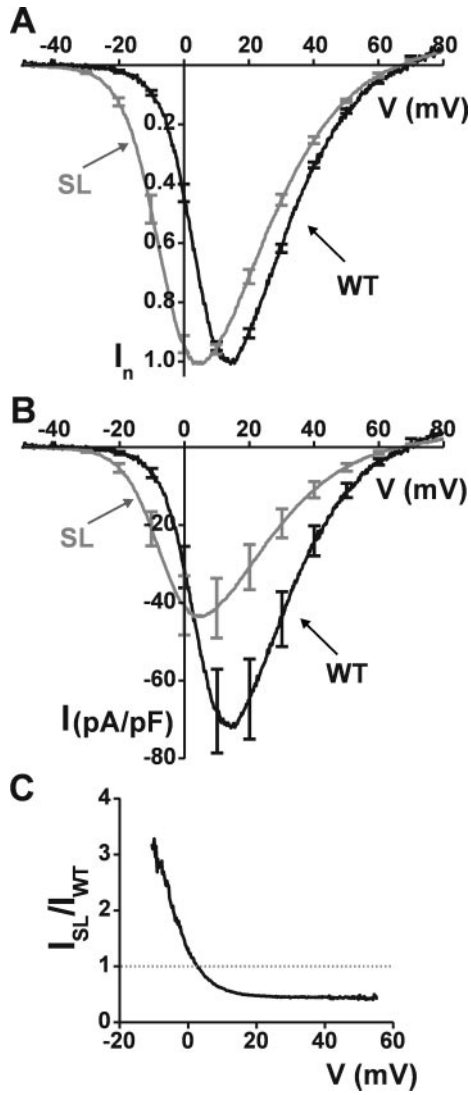

FIG. 2. **Mutation S218L leads to an increased whole cell current density in a broad voltage range in HEK293 cells expressing human $Ca_V2.1$ channels.** Whole cell recordings (5 mM Ba^{2+} as charge carrier) were performed on HEK293 cells cotransfected with human WT or mutant S218L $Ca_V2.1$ α_1 subunits together with human $\alpha_{2b}\delta$ and β_{2e} subunits. Holding potential = −80 mV. *A*, normalized whole cell current density, I_n, measured during voltage ramps in cells expressing WT (n = 15) or S218L mutant (n = 7) human $Ca_V2.1$ channels. Fitting the curves with Equation 1 gives $V_{1/2}$ values of +5.0 and −5.7 mV for the WT and the S218L mutant, respectively. *B*, whole cell current densities as a function of voltage in cells expressing WT or mutant human $Ca_V2.1$ channels. The average normalized current densities measured during voltage ramps (shown in *A*) were multiplied by the average maximal current density measured in 31 cells expressing the WT (71.6 ± 11.3 pA/pF) and 26 cells expressing the S218L mutant (43.2 ± 8 pA/pF). *C*, ratio of mutant and WT current densities (I_{SL}/I_{WT}) as a function of voltage. The ratio reaches a constant value independent of voltage $(I_{SL}/I_{WT})_{sat}$ = 0.45 at voltages where the open probability of both WT and mutant channel reaches the maximum value. From $(I_{SL}/I_{WT})_{sat}$ one can obtain an estimate of N_{SL}/N_{WT}, the ratio of the density of functional channels in the membrane of cells expressing the S218L mutant and the WT channels (see "Results").

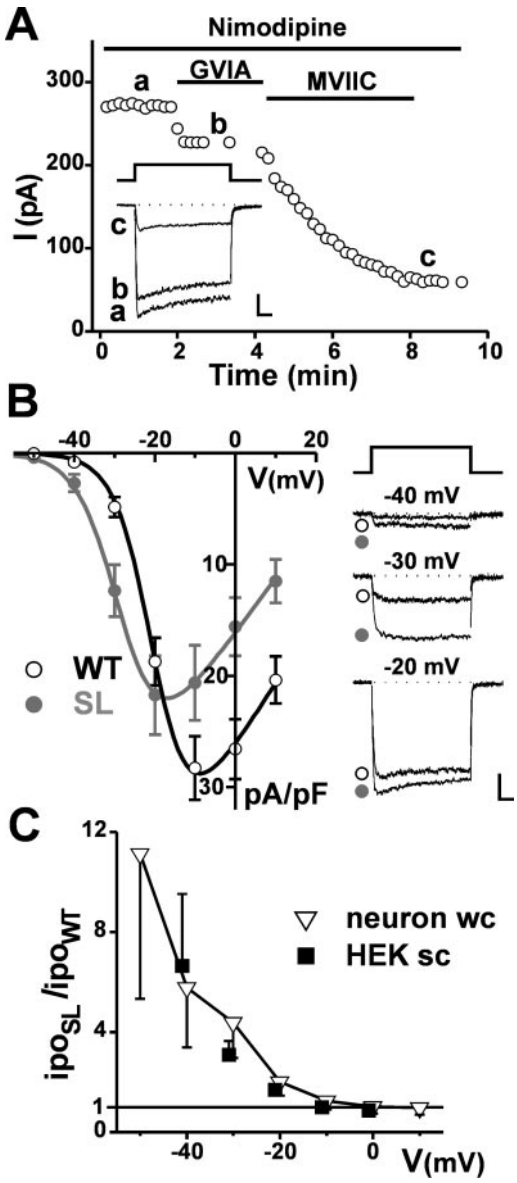

FIG. 3. **Mutation S218L leads to an increased $Ca_V2.1$ current density in a broad voltage range in $Ca_V2.1$ $\alpha_1^{-/-}$ neurons transfected with human $Ca_V2.1$ α_1 subunits.** Whole cell recordings (5 mM Ba^{2+}) were made on cerebellar granule cells of $Ca_V2.1$ $\alpha_1^{-/-}$ mouse transfected with WT or S218L mutant human $Ca_V2.1$ α_1 subunits. *A*, plot of peak current *versus* time for a representative experiment on a neuron transfected with S218L $Ca_V2.1$ α_1 subunits. Depolarizations at −20 mV were delivered every 10 s from −80 mV. ω-conotoxin GVIA (1 μM) and ω-conotoxin MVIIC (3 μM) were applied sequentially, in the continuous presence of nimodipine (5 μM). *Inset*, representative traces taken at times *a*, *b*, and *c*. $Ca_V2.1$ currents were obtained as the difference between traces at times *b* and *c*. *Scale bars*, 20 ms and 50 pA. *B*, $Ca_V2.1$ current density as a function of voltage in neurons expressing WT or S218L mutant $Ca_V2.1$ α_1 subunits. The average normalized current densities (n = 10 for both WT and S218L) were multiplied by the average maximal current density measured in 16 neurons expressing the WT (29.1 ± 2.9 pA/pF) and 20 neurons expressing the S218L mutant (22.7 ± 3.7 pA/pF). *Inset* on the *right*, pooled WT (n = 9) and S218L (n = 10) current traces at −40, −30, and −20 mV. *Scale bars*, 5 pA/pF and 20 ms. *C*, single channel Ba^{2+} influx of the S218L mutant relative to that of the WT channel, ip_{oSL}/ip_{oWT}, as a function of voltage, obtained from the current densities in *B*, as described under "Results" (*inverted triangles*; *wc* = whole cell). For comparison, the figure also shows the values of ip_{oSL}/ip_{oWT}, measured in HEK293 cells with 90 mM Ba^{2+} as charge carrier (*squares*; *sc* = single channel): these values were shifted toward hyperpolarized voltages of 51 mV to account for the difference in surface potential with respect to the whole cell recording solution with 5 mM Ba^{2+} and for the difference in the voltage range of activation of $Ca_V2.1$ channels expressed in neurons or HEK293 cells (see Figs. 2 and 3 and "Results").

Interestingly, we confirm here for the (−VEA) splicing variant of the $Ca_V2.1$ α_1 human subunit the previous finding obtained for the (+VEA) variant (13) of a more than 20 mV difference in the voltage range of activation of $Ca_V2.1$ channels expressed in neurons or HEK293 cells (compare $V_{1/2}$ = +5 mV in HEK293 cells with $V_{1/2}$ = −19.5 mV in neurons, obtained from fitting the *I-V* curves in Figs. 2 and 3, respectively). However, as found previously for the other FHM-1 mutants, the hyperpolarized shift in the voltage range of activation of mutant S218L channels expressed in neurons was similar to that of the same mutant channels expressed in HEK293 cells. Further support for the conclusion that the alterations in single channel function produced by the S218L mutation are similar in neurons and HEK293 cells comes from the comparison in Fig. 3*C* of the relative increase in single channel Ba^{2+} influx of the S218L mutant, ip_{oSL}/ip_{oWT}, obtained from direct single channel measurements in HEK293 cells and of the same ratio in neurons, calculated from the ratio of the P/Q current densities of mutant and WT channels, I_{SL}/I_{WT}, divided by the ratio of the density of channels in the membrane, N_{SL}/N_{WT}. N_{SL}/N_{WT} in neurons was estimated, as described above, from the value of $(I_{SL}/I_{WT})_{sat}$ (obtained from I_{SL}/I_{WT} at 0 and 10 mV = 0.58 ± 0.11) (see Ref. 13). In Fig. 3*C*, the values of ip_{oSL}/ip_{oWT}, measured in HEK293 cells with 90 mM Ba^{2+} as charge carrier, were shifted toward hyperpolarized voltages of 51 mV, to account for the difference in surface potential with respect to the whole cell recording solution with 5 mM Ba^{2+} (26 mV; see Ref. 13) and for the difference in the voltage range of activation of $Ca_V2.1$ channels expressed in neurons or HEK293 cells, mentioned above (see Figs. 2 and 3 and Ref. 13). The strikingly similar values of ip_{oSL}/ip_{oWT} in HEK293 cells and neurons at all voltages indicate that the S218L mutation produces a similar increase of single channel Ba^{2+} influx in the two expression systems. In neurons, with nearly physiological concentrations of charge carrier, the single channel influx through the S218L mutant is larger than through the WT channel for $V < -10$ mV, and the relative gain of function of the mutant channel increases with more negative voltages.

Given the similar gain of function of mutant S218L channels in neurons and HEK293 cells, the smaller $Ca_V2.1$ whole cell current density at $V > -20$ mV in neurons expressing the S218L mutant compared with that in neurons expressing the WT channel must be mainly the result of a reduced density of functional channels in the membrane. A reduced whole cell P/Q current density at $V > -20$ mV and a reduced density of functional channels in the membrane were consistent properties of the four human FHM-1 mutants expressed previously in cerebellar granule cells of $Ca_V2.1$ $\alpha_1^{-/-}$ mice (13), including the R192Q mutant that in HEK293 cells showed the opposite properties (14). Compared with S218L, these FHM-1 mutants showed a larger reduction in the density of functional channels and/or a smaller gain in single channel influx; as a consequence, their P/Q current density was similar to that of the WT channel at low voltages, in contrast with the larger current density of the S218L mutant (Fig. 3*B*).

To complete the functional characterization of the S218L mutant, we studied its inactivation properties in HEK293 cells expressing human S218L $Ca_V2.1$ α_1, $\alpha_{2b}\delta$, and β_{1b} subunits. Investigation of the kinetics of channel inactivation during long depolarizations and during trains of short pulses and of the kinetics of recovery from inactivation revealed some interesting features distinguishing the S218L mutant from the WT channel and from the other FHM-1 mutants.

Different kinetics of inactivation of the S218L mutant and the WT channel were revealed by comparing the average normalized current traces recorded during depolarizations lasting

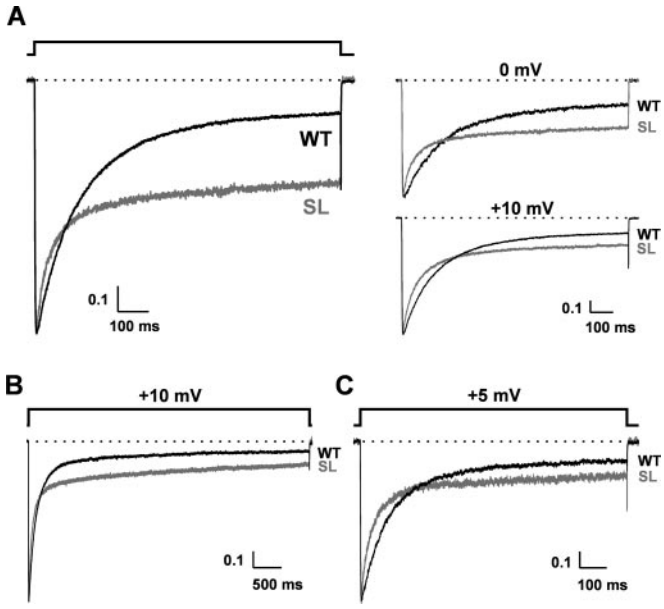

FIG. 4. **Mutation S218L affects both fast and slow inactivation of human $Ca_V2.1$ channels and decreases the extent of inactivation during long depolarizations.** Whole cell recordings were made on HEK293 cells cotransfected with human WT or mutant S218L $Ca_V2.1$ α_1 subunits together with human $\alpha_{2b}\delta$ and β_{1b} subunits. Holding potential = −80 mV. *A*, *left panel*, average normalized current traces of WT and S218L mutant human $Ca_V2.1$ channels recorded during depolarizations of 1 s at voltages close to the peak of the *I-V* curves (0 mV for the SL, $n = 18$; and +10 mV for the WT, $n = 12$) in the *left panel* and at 0 mV (WT, $n = 7$; SL, $n = 18$) and +10 mV (WT, $n = 12$; SL, $n = 12$) for both WT and mutant, in the *right panels*. 5 mM Ba^{2+} was the charge carrier. The current remaining at the end of the depolarization at 0 mV was 21% of the pooled peak current for the WT and 40% for the mutant; at +10 mV it was 13% for the WT and 23% for the mutant. For the WT channel, the time course of inactivation was best fit with two exponential components with time constants (and relative amplitudes) of 146 ms (65%) and 1.9 s (35%) at 0 mV and 129 ms (75%) and 1.5 s (25%) at +10 mV. For the S218L mutant, three exponential components were necessary for the best fit of the time course of inactivation, with time constants of 26 ms (27%), 103 ms (24%), and 5.3 s (49%) at 0 mV, and 33 ms (34%), 126 ms (36%), and 4 s (30%) at +10 mV. *B*, average normalized current traces of WT and S218L mutant human $Ca_V2.1$ channels recorded during depolarizations of 5 s at +10 mV, with 5 mM Ba^{2+} as charge carrier (WT, $n = 10$; SL, $n = 9$). The current remaining at the end of the depolarization was 6% of the pooled peak current for the WT and 14% for the mutant. The time course of inactivation was best fit with three exponentials with time constants of 108 ms (65%), 339 ms (23%), and 7.3 s (12%) for the WT, and 54 ms (58%), 291 ms (16%), and 8.7 s (26%) for S218L. *C*, average normalized current traces of WT and S218L mutant human $Ca_V2.1$ channels recorded during depolarizations of 1 s at +5 mV, with 2 mM Ca^{2+} as charge carrier ($n = 9$ for both WT and S218L). The average values of the peak Ca^{2+} current densities of the pooled traces were not significantly different for WT and S218L. The current remaining at the end of the depolarization was 12% of the peak pooled current for the WT and 22% for the mutant. The time course of inactivation was best fit with two exponential components with time constants (and relative amplitudes) of 97 ms (78%) and 1.5 s (22%) for the WT channel and with three exponential components with time constants of 14 ms (22%), 61 ms (48%), and 3.1 s (30%) for the S218L mutant.

1 s at voltages close to the peak of the *I-V* curves (0 mV for the S218L and 10 mV for the WT) (Fig. 4*A*, *left panel*). About half of the S218L Ba^{2+} current inactivated quite rapidly (more rapidly than the WT), whereas the other half inactivated very slowly and gave rise to a large residual current remaining at the end of the long depolarization (about three times larger than for the WT channel). In 1 s, only 59 ± 3% ($n = 18$) of the S218L current inactivated, in contrast with 87 ± 2% ($n = 12$) of the WT current. Similar differences in inactivation kinetics were found when average normalized current traces recorded at the same voltage (either 0 or 10 mV) for both WT and mutant channels were considered (Fig. 4*A*, *right panels*). It is interesting to compare the kinetics of inactivation of S218L mutant and WT channels during long depolarizations at these voltages because during CSD (the phenomenon underlying migraine aura (5)), the membrane potential of cortical neurons becomes almost zero for about 1 min (24). For the WT channel, the time course of inactivation at 0 mV was best fit with two exponential components with time constants (and relative amplitudes) of 150 ± 11 ms (66 ± 3%) and 2.31 ± 0.37 s (34 ± 3%). On the other hand, for the S218L mutant, three exponential components were necessary for the best fit of the time course of inactivation, with time constants of 23 ± 2 ms (25 ± 3%), 108 ± 10 ms (28 ± 3%), and 6.4 ± 0.9 s (47 ± 3%). The residual current remaining after 1 s at 0 mV was 41 ± 3% of the peak current ($n = 18$), almost twice that remaining for the WT channel (21 ± 3%, $n = 7$). Similar differences in inactivation kinetics between S218L and WT were observed during depolarizations of 1 s at 10 mV (*e.g.* about 1.8 times larger residual current for the S218L than for the WT channel). When the duration of the depolarization was prolonged to 5 s, the relative difference in residual current at the end of the depolarization was further enhanced: the current remaining after 5 s at 10 mV was 2.3 times larger for the S218L mutant than for the WT (Fig. 4*B*; a similar difference was observed at 0 mV, not shown). In conclusion, mutation S218L appears to affect both slow inactivation (increasing its contribution) and fast inactivation (making it more rapid). As a result, during long depolarizations the extent of inactivation of the S218L mutant was smaller than that of the WT channel (the more the more prolonged the depolarization), whereas during relatively short depolarizations (<200 ms) the extent of inactivation of the mutant was actually larger.

Similar differences in kinetics of inactivation between S218L and WT channels during long depolarizations were observed using 2 mM Ca^{2+} as charge carrier, with 0.5 mM EGTA (rather than 10 mM) in the intracellular solution to highlights Ca^{2+}-dependent inactivation (25) (Fig. 4*C*). In these more physiological conditions, the S218L mutant still showed a component of current that inactivated very slowly, and the residual current of the mutant was still about twice that of the WT after long depolarizations of 1 s (at 5 mV, 22 ± 3% for S218L and 12 ± 1% for WT, $n = 9$).

Moreover, similarly different kinetics of inactivation between S218L mutant and WT channels were found during trains of 100 short pulses (10 ms, 0 mV) delivered at 50 Hz (Fig. 5*A*). The S218L mutant inactivated more than the WT channel during relatively short trains (<20 pulses corresponding to <200 ms total depolarization time) but inactivated less than the WT during long trains. After 100 pulses only 53 ± 3% ($n = 12$) of the S218L Ba^{2+} current inactivated, in contrast with 70 ± 3% ($n = 6$) of the WT current, and the current during the last pulse at 0 mV at the end of the train was 1.6 times larger for the mutant than for the WT. Thus, despite the faster inactivation of the S218L mutant during the short pulses, the ratio of the mutant and WT currents at the end of the train of pulses (of cumulative duration 100 × 0.01 = 1 s) was similar to that at the end of a 1-s depolarization.

This finding and in general the similarity in the relative kinetics of inactivation of the mutant and WT channels during long depolarizations and during trains of short pulses (Figs. 4*A* and 5*A*) can be explained by the faster recovery from inactivation of the S218L mutant compared with the WT channel shown in Fig. 5*B*. For the WT channel, the average time course of the recovery from inactivation (after a 1-s depolarization) was best fit with two exponential components with time con-

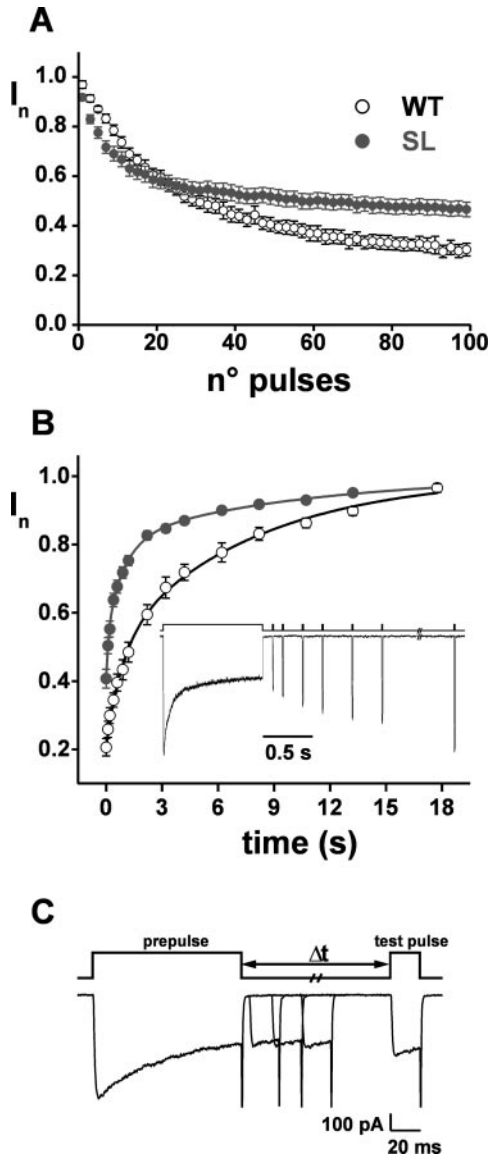

FIG. 5. **Mutation S218L increases the rate of recovery from inactivation of human $Ca_V2.1$ channels.** Whole cell recordings (5 mM Ba^{2+} as charge carrier) were made on HEK293 cells cotransfected with human WT or mutant S218L $Ca_V2.1$ α_1 subunits together with human $\alpha_{2b}\delta$ and β_{1b} subunits. Holding potential = −80 mV. *A*, average normalized current, I_n, of WT and S218L mutant human $Ca_V2.1$ channels measured during 50-Hz trains of 100 pulses of 10-ms duration to 0 mV (cumulative duration 100 × 0.01 = 1 s). The current measured during the successive pulses in the train was normalized to that of the first test pulse. The current of the last pulse was 30% that of the first pulse for the WT channel (n = 6) and 47% for the mutant (n = 12). The time course of the current decay during the train was best fit with two exponential components with time constants (and relative amplitudes) of 217 ms (63%) and 4.7 s (37%) for the WT channel and with three exponential components with time constants of 14 ms (8%), 93 ms (35%), and 4.9 s (57%) for the mutant. *B*, time course of recovery from inactivation of WT (n = 7) and S218L mutant (n = 18) human $Ca_V2.1$ channels after a 1-s depolarization to 0 mV. Recovery from inactivation was measured applying short (10 ms) test depolarizations to 0 mV at various times after the 1-s conditioning depolarization. Representative current traces of the S218L channel recorded using this protocol are shown in the *inset*. The peak currents measured during the test depolarizations were normalized to the peak current of the conditioning depolarization. *Lines* through the *data points* represent best fits with two exponential components for WT and three exponential components for S218L (see parameters under "Results"). *C*, representative current traces of the S218L channel recorded during a double pulse protocol designed to monitor the extent of channel inactivation at early time points after a 100-ms prepulse to 0 mV, as in Ref. 28. The test pulse traces, recorded 5, 20, 40, and 100 ms after the prepulse, show that recovery from inactivation started immediately after the prepulse.

stants (and relative amplitudes) of 0.88 s (36%) and 7.62 s (64%), whereas for the S218L mutant, three exponential components were necessary, with time constants of 0.17 s (24%), 1.00 s (44%), and 10.3 s (32%). The mutant channel recovered from inactivation more rapidly than the WT channel, as a consequence of both a smaller amplitude of the slow component of recovery and the presence of a component of current recovering very rapidly (more than five times faster than the WT). As a result, the time necessary to recover 80% of the current was more than three times shorter for the S218L mutant than for the WT (less than 2 s compared with 6 s at −80 mV). Although a considerably faster rate of recovery from inactivation was reported previously for other two FHM-1 mutants (V714A and I1811L) (11, 14), the combination of both a much faster rate of recovery from inactivation and a much smaller extent of inactivation during long depolarizations is unique to the S218L mutant. In general, the other FHM-1 mutations analyzed did not show consistent effects on the kinetics of inactivation of $Ca_V2.1$ channels, and their variable effects were usually small: depending on the mutation, inactivation during train of pulses (or during long depolarizations) was increased, decreased, or unaffected (11, 12, 14, 15).

For both the WT channel and the S218L mutant, the amount of inactivation during a long depolarization was similar, or if anything larger, than during a train of short pulses of comparable cumulative duration. In contrast, a larger inactivation during trains of action potentials was reported previously for a different rat $Ca_V2.1$ isoform and was attributed to preferential inactivation from closed states (26). Using a two-pulse protocol as in Ref. 26 to monitor recovery from inactivation of mutant and WT channels at early time points, we did not find evidence for a phase of further decline of the current before recovery (Fig. 5*C*). Therefore, in contrast to the rat isoform (26), our human $Ca_V2.1$ isoform does not further inactivate during the repolarization period, and closed state inactivation seems to play a minor role in its kinetics of inactivation during trains of short pulses.

Finally, we investigated the effect of the S218L mutation on steady-state inactivation of human $Ca_V2.1$ channels by measuring WT and mutant currents at different holding potentials, V_h, as illustrated in the representative experiment in Fig. 6. The almost identical inactivation curves for WT and S218L channels in Fig. 6 show that mutation S218L does not affect steady-state inactivation of $Ca_V2.1$ channels, as found previously for most FHM-1 mutations (11, 12, 14, 15).

DISCUSSION

The S218L mutation in the IS4-IS5 linker of the human $Ca_V2.1$ α_1 subunit produces a severe clinical phenotype, in which typical attacks of FHM triggered by minor head trauma are frequently followed, after a lucid interval, by deep (even fatal) coma and long lasting severe cerebral edema. Other common symptoms are ataxia and cerebral and/or cerebellar atrophy (18, 19). Impairment of consciousness is a known but relatively rare associated symptom of FHM-1 attacks; however, it is usually short lived and less severe than in S218L patients, and there is not such dramatic delayed association with minor head trauma (2). On the other hand, a syndrome characterized by severe, even fatal, cerebral edema and coma occurring after a lucid interval is a possible complication of minor head trauma in children (19, 27).

We have studied the functional consequences of mutation S218L on human $Ca_V2.1$ channels expressed in HEK293 cells and in neurons from $Ca_V2.1$ $\alpha_1^{-/-}$ mice by combining single channel and whole cell patch clamp recordings. Our data show that mutation S218L produces a shift to lower voltages of the single channel activation curve and a consequent increase of

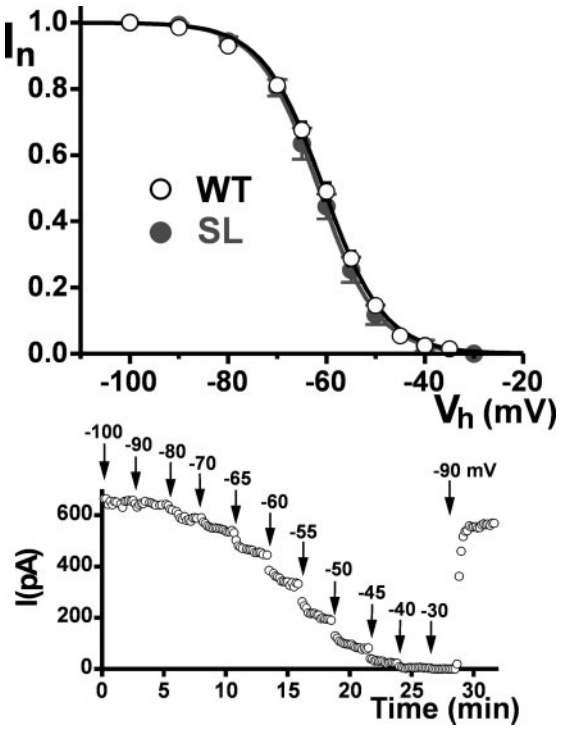

FIG. 6. **Mutation S218L does not affect steady-state inactivation of human $Ca_V2.1$ channels.** Whole cell recordings (5 mM Ba^{2+} as charge carrier) were made on HEK293 cells cotransfected with human WT or mutant S218L $Ca_V2.1$ α_1 subunits together with human $\alpha_{2b}\delta$ and β_{1b} subunits. Peak normalized current, I_n, is shown as a function of holding potential, V_h, for WT ($n = 6$) and S218L ($n = 6$) human $Ca_V2.1$ channels. Cells were maintained for about 2.5 min at each holding potential, and the peak current was monitored continuously by test pulses every 10 s, as illustrated in the representative experiment in the *bottom panel*; the *arrows* show the time at which V_h was changed to the indicated value. For each cell, peak currents measured at the end of each period at different V_h were normalized with respect to the maximal current at −100 mV. Average values of I_n as a function of V_h were best fit by Boltzmann distributions of the form $I_n = (1 + \exp(V - V_{1/2})/k)^{-1}$, with $V_{1/2} = -61$ mV ($k = 6.2$) for WT and $V_{1/2} = -62$ mV ($k = 6.0$) for S218L.

both single channel and whole cell ion influx through human $Ca_V2.1$ channels expressed in either neurons or HEK293 cells. This finding confirms and supports the conclusion that a consistent effect of FHM-1 mutations is to produce gain of function of human $Ca_V2.1$ channels, mainly because of a shift to lower voltages of channel activation (13, 17). Compared with the other FHM-1 mutations, S218L is one of the mutations that produces the largest shift to lower voltages of channel activation and the largest gain of function especially for small depolarizations, which are insufficient to open the WT channel. In cerebellar granule cells mutant S218L channels open and carry significant current at voltages (−60 to −50 mV) close to the resting potential of many neurons. The particularly large increase in single channel Ca^{2+} influx of the S218L mutant results in an increased whole cell P/Q current density (at $V <$ −20 mV in neurons), despite the reduced density of functional mutant channels in the membrane. In contrast, for the four FHM-1 mutants expressed previously in neurons, the reduced density of functional channels in the membrane prevailed over the single channel gain of function resulting in an unaltered or reduced P/Q current density at the same voltages (13, 16).

However, the recent analysis of $Ca_V2.1$ channels in neurons of the R192Q knock-in mouse expressing mutant channels at their endogenous level (17) suggests that the alterations in the number of functional channels in the membrane produced by the FHM-1 mutations in transfected cells (13, 14) are probably an artifact caused by overexpression. In fact, in contrast with the reduced whole cell P/Q current density found in transfected neurons overexpressing the R192Q mutant (13, 16), in both cerebellar granule cells in culture (17) and freshly dissociated cortical pyramidal neurons (28) of the R192Q knock-in mouse, the whole cell P/Q current density was larger than that in WT neurons in a broad voltage range and similar to that of WT neurons at higher voltages. The changes in P/Q current density measured in the knock-in neurons are those expected if mutant mouse $Ca_V2.1$ channels have a gain-of-function phenotype similar to that established for mutant human $Ca_V2.1$ channels (14, 13) and if the number of functional channels in the membrane is not altered by the mutation. The knock-in data suggest that one may obtain misleading answers using transfected neurons overexpressing FHM-1 mutants to study the effect of the mutations on cellular functions that depend on the number of functional channels in the membrane, such as neuronal excitability or synaptic transmission. Indeed, Cao *et al.* (16) found an unaltered synaptic transmission and a decreased contribution of P/Q channels in controlling release at synapses between hippocampal neurons transfected with R192Q $Ca_V2.1$ α_1 subunits. In contrast, the R192Q knock-in mice showed increased neurotransmission at the neuromuscular junction in conditions of low release probability (17) and enhanced glutamate release from cortical neurons in culture.[3] Moreover, in agreement with the particularly low threshold of activation of S218L human $Ca_V2.1$ channels reported here, preliminary data obtained on a recently generated S218L knock-in mouse show a striking increase of spontaneous release at the neuromuscular junction (much larger than that of the R192Q mouse) (29).

Besides leading to a particularly large increase in Ca^{2+} influx at low voltages, mutation S218L strongly affects the kinetics of inactivation of human $Ca_V2.1$ channels. On one hand it makes fast inactivation more rapid, and on the other hand it increases the contribution of slow inactivation, introducing a large component of current that inactivates very slowly. During long depolarizations, at voltages that are attained during CSD, the extent of inactivation of the S218L channel is considerably smaller than that of the WT channel. Moreover, the rate of recovery from inactivation of the S218L mutant is considerably faster. Compared with the other FHM-1 mutants, the combination of both a much smaller extent of inactivation during long depolarizations and a much faster rate of recovery from inactivation are unique to the S218L mutant.

Can the specific functional effects of the S218L mutation account for the severe clinical phenotype? Neuroimaging findings indicate that migraine aura is caused by CSD, a wave of sustained strong neuronal depolarization, which progresses slowly across the cortex, generating a transient intense spike activity followed by a long lasting neural suppression (5, 30–32). Animal studies have shown that CSD can activate the meningeal trigeminal nociceptive afferents and evoke alterations in the meninges and brainstem consistent with the development of headache (33). These studies support the idea that CSD may initiate migraine attacks (5). Interestingly, the R192Q knock-in mice show an increased susceptibility to CSD (17). Gain of function of $Ca_V2.1$ channels leads to a lower threshold for CSD induction, an increased velocity of propagation, and a longer duration of the CSD depolarization *in vivo* (17). On the other hand, loss of function of $Ca_V2.1$ channels in the natural *Cacna1a* mutant *leaner* mouse (34, 35) leads to a higher threshold for CSD induction, a lower velocity of propagation, and a shorter duration of the CSD depolarization *in vivo* (36). Similar effects on threshold, propagation, and duration of

[3] A. Tottene and D. Pietrobon, unpublished observations.

CSD *in vivo* are produced by NMDA antagonists, in a dose-dependent manner (24, 37).

The initiation of the positive feedback cycle that almost zeros the neuronal membrane potential and ignites CSD depends critically on the local increase above a critical value of the K^+ concentration in the narrow space surrounding cortical neurons and the activation of a sustained net inward current in apical dendrites (24).The pivotal role played by both NMDA receptors and $Ca_V2.1$ channels in CSD induction is consistent with a positive feedback mechanism in which excessive $Ca_V2.1$-dependent release of glutamate from synaptic terminals depolarized by high K^+ and consequent activation of NMDA receptors leads to further depolarization of the postsynaptic membrane, further increase in K^+ in the extracellular space, further release of glutamate, further activation of the NMDA receptor, and so on (38).

Enhanced susceptibility to CSD in FHM-1 can be explained, considering that a weaker depolarizing stimulus and a lower increase of extracellular K^+ are necessary to activate mutant synaptic $Ca_V2.1$ channels and to release enough glutamate to initiate the positive feedback cycle leading to CSD. Thus, a weak depolarizing stimulus, as a minor head trauma, which is without consequences in healthy individuals, may be able to initiate CSD in FHM-1 patients. Although minor head trauma is a frequent triggering factor of FHM-1 attacks (2), the dramatic delayed association with cerebral edema and coma is unique to S218L patients. We propose that the severe phenotype produced by S218L channels may be the result of their unique combination of a particularly low threshold of activation with a particularly slow inactivation during the long CSD depolarization. Our working hypothesis is that because of these unique properties, minor head trauma may lead to a longer duration of CSD in S218L patients. A longer duration of CSD and prolonged activation of NMDA receptors may have indirect damaging effects, *e.g.* because of excessive accumulation of intracellular Ca^{2+} or production of nitric oxide, arachidonic acid, and reactive oxygen species, which among other effects may lead to impairment of the blood-brain barrier (39) and enhancement of both vasogenic and cytotoxic edema. An additional effect might be impairment of mitochondrial function and ATP supply, which may lead to repetitive CSDs and enhanced neuronal vulnerability after minor head trauma. This hypothesis was suggested by the interesting findings that sublethal stretch applied to cortical neurons in culture induced mitochondrial dysfunction and a consequent delayed long lasting small neuronal depolarization and enhanced vulnerability to glutamate challenges (40–42). Induction of these alterations required depolarization-induced Ca^{2+} entry, glutamate release, and activation of NMDA receptors. The recently generated S218L knock-in mouse will allow testing of our working hypotheses.

Acknowledgments—We thank Dr. J. Striessnig (University of Innsbruck, Austria) for the $Ca_V2.1$ α_1 cDNA, Dr. M. Williams (Merck Research Laboratories, San Diego, CA) for the $\alpha_2\delta$, β_{2e}, and β_{1b} cDNAs. We thank L. Broos (Leiden University Medical Center, The Netherlands) for technical assistance on generating the mutant construct and E. Andrini and S. Pagnutti for help in performing some of the electrophysiological experiments.

REFERENCES

1. Thomsen, L. L., Eriksen, M. K., Roemer, S. F., Andersen, I., Olesen, J., and Russell, M. B. (2002) *Brain* **125,** 1379–1391
2. Ducros, A., Denier, C., Joutel, A., Cecillon, M., Lescoat, C., Vahedi, K., Darcel, F., Vicaut, E., Bousser, M. G., and Tournier-Lasserve, E. (2001) *N. Engl. J. Med.* **345,** 17–24
3. Ophoff, R. A., Terwindt, G. M., Vergouwe, M. N., van Eijk, R., Oefner, P. J., Hoffman, S. M. G., Lamerdin, J. E., Mohrenweiser, H. W., Bulman, D. E., Ferrari, M., Haan, J., Lindhout, D., van Hommen, G.-J. B., Hofker, M. H., Ferrari, M. D., and Frants, R. R. (1996) *Cell* **87,** 543–552
4. Westenbroek, R. E., Sakurai, T., Elliott, E. M., Hell, J. W., Starr, T. V. B., Snutch, T. P., and Catterall, W. A. (1995) *J. Neurosci.* **15,** 6403–6418
5. Pietrobon, D., and Striessnig, J. (2003) *Nat. Rev. Neurosci.* **4,** 386–398
6. Dunlap, K., Luebke, J. I., and Turner, T. J. (1995) *Trends Neurosci.* **18,** 89–98
7. Pineda, J. C., Waters, R. S., and Foehring, R. C. (1998) *J. Neurophysiol.* **79,** 2522–2534
8. Haan, J., Kors, E. E., van den Maagdenberg, A. M., Vanmolkot, K. R., Terwindt, G. M., Frants, R. R., and Ferrari, M. D. (2004) *Curr. Pain Headache Rep.* **8,** 238–243
9. Kors, E. E., Melberg, A., Vanmolkot, K. R., Kumlien, E., Haan, J., Raininko, R., Flink, R., Ginjaar, H. B., Frants, R. R., Ferrari, M. D., and van den Maagdenberg, A. M. (2004) *Neurology* **63,** 1136–1137
10. Alonso, I., Barros, J., Tuna, A., Seixas, A., Coutinho, P., Sequeiros, J., and Silveira, I. (2004) *Clin. Genet.* **65,** 70–72
11. Kraus, R. L., Sinnegger, M. J., Glossmann, H., Hering, S., and Striessnig, J. (1998) *J. Biol. Chem.* **273,** 5586–5590
12. Kraus, R. L., Sinnegger, M., Koschak, A., Glossmann, H., Stenirri, S., Carrera, P., and Striessnig, J. (2000) *J. Biol. Chem.* **275,** 9239–9243
13. Tottene, A., Fellin, T., Pagnutti, S., Luvisetto, S., Striessnig, J., Fletcher, C., and Pietrobon, D. (2002) *Proc. Natl. Acad. Sci. U. S. A.* **99,** 13284–13289
14. Hans, M., Luvisetto, S., Williams, M. E., Spagnolo, M., Urrutia, A., Tottene, A., Brust, P. F., Johnson, E. C., Harpold, M. M., Stauderman, K. A., and Pietrobon, D. (1999) *J. Neurosci.* **19,** 1610–1619
15. Mullner, C., Broos, L. A., van den Maagdenberg, A. M., and Striessnig, J. (2004) *J. Biol. Chem.* **279,** 51844–51850
16. Cao, Y. Q., Piedras-Renteria, E. S., Smith, G. B., Chen, G., Harata, N. C., and Tsien, R. W. (2004) *Neuron* **43,** 387–400
17. van den Maagdenberg, A. M., Pietrobon, D., Pizzorusso, T., Kaja, S., Broos, L. A., Cesetti, T., van de Ven, R. C., Tottene, A., van der Kaa, J., Plomp, J. J., Frants, R. R., and Ferrari, M. D. (2004) *Neuron* **41,** 701–710
18. Fitzsimons, R. B., and Wolfenden, W. H. (1985) *Brain* **108 (Pt 3),** 555–577
19. Kors, E. E., Terwindt, G. M., Vermeulen, F. L., Fitzsimons, R. B., Jardine, P. E., Heywood, P., Love, S., van den Maagdenberg, A. M., Haan, J., Frants, R. R., and Ferrari, M. D. (2001) *Ann. Neurol.* **49,** 753–760
20. Wappl, E., Koschak, A., Poteser, M., Sinnegger, M. J., Walter, D., Eberhart, A., Groschner, K., Glossmann, H., Kraus, R. L., Grabner, M., and Striessnig, J. (2002) *J. Biol. Chem.* **277,** 6960–6966
21. Grabner, M., Wang, Z., Hering, S., Striessnig, J., and Glossmann, H. (1996) *Neuron* **16,** 207–218
22. Fletcher, C. F., Tottene, A., Lennon, V. A., Wilson, S. M., Dubel, S. J., Paylor, R., Hosford, D. A., Tessarollo, L., McEnery, M. W., Pietrobon, D., Copeland, N. G., and Jenkins, N. A. (2001) *FASEB J.* **15,** 1288–1290
23. Neher, E. (1992) *Methods Enzymol.* **207,** 123–131
24. Somjen, G. G. (2001) *Physiol. Rev.* **81,** 1065–1096
25. Liang, H., DeMaria, C. D., Erickson, M. G., Mori, M. X., Alseikhan, B. A., and Yue, D. T. (2003) *Neuron* **39,** 951–960
26. Patil, P. G., Brody, D. L., and Yue, D. T. (1998) *Neuron* **20,** 1027–1038
27. Snoek, J. W., Minderhoud, J. M., and Wilmink, J. T. (1984) *Brain* **107,** 15–36
28. Shapovalova, M., Matiello, S., Tottene, A., van den Maagdenberg, A. M., and Pietrobon, D. (2004) *Society for Neuroscience 34th Annual Meeting*, October 23–27, 2004, San Diego, 848.9 (abstr.)
29. Kaja, S., van de Ven, R. C., Broos, L. A., Frants, R. R., Ferrari, M. D., van den Maagdenberg, A. M., and Plomp, J. J. (2004) *Society for Neuroscience 34th Annual Meeting*, October 23–27, 2004, San Diego, 593.4 (abstr.)
30. Hadjikhani, N., Sanchez del Rio, M., Wu, O., Schwartz, D., Bakker, D., Fischl, B., Kwong, K. K., Cutrer, F. M., Rosen, B. R., Tootell, R. B. H., Sorensen, A. G., and Moskowitz, M. A. (2001) *Proc. Natl. Acad. Sci.* **98,** 4687–4692
31. Lauritzen, M. (1994) *Brain* **117,** 199–210
32. Bowyer, S. M., Aurora, K. S., Moran, J. E., Tepley, N., and Welch, K. M. (2001) *Ann. Neurol.* **50,** 582–587
33. Bolay, H., Reuter, U., Dunn, A. K., Huang, Z., Boas, D. A., and Moskowitz, M. A. (2002) *Nat. Med.* **8,** 136–142
34. Fletcher, C. F., Lutz, C. M., O'Sullivan, T. N., Shaughnessy, J. D. J., Hawkes, R. H., Frankel, W. N., Copeland, N. G., and Jenkins, N. A. (1996) *Cell* **87,** 607–617
35. Pietrobon, D. (2002) *Mol. Neurobiol.* **25,** 31–50
36. Ayata, C., Shimizu-Sasamata, M., Lo, E. H., Noebels, J. L., and Moskowitz. (2000) *Neuroscience* **95,** 639–645
37. Marrannes, R., Willems, R., De Prins, E., and Wauquier, A. (1988) *Brain Res.* **457,** 226–240
38. Pietrobon, D. (2005) *The Neuroscientist*, in press
39. Gursoy-Ozdemir, Y., Qiu, J., Matsuoka, N., Bolay, H., Bermpohl, D., Jin, H., Wang, X., Rosenberg, G. A., Lo, E. H., and Moskowitz, M. A. (2004) *J. Clin. Invest.* **113,** 1447–1455
40. Tavalin, S. J., Ellis, E. F., and Satin, L. S. (1995) *J. Neurophysiol.* **74,** 2767–2773
41. Tavalin, S. J., Ellis, E. F., and Satin, L. S. (1997) *J. Neurophysiol.* **77,** 632–638
42. Arundine, M., Aarts, M., Lau, A., and Tymianski, M. (2004) *J. Neurosci.* **24,** 8106–8123